The 2010 IEEE/RSJ International Conference on
Intelligent Robots and Systems
October 18-22, 2010, Taipei, Taiwan

Time-Delayed Bilateral Teleoperation with Force Estimation for n-DOF Nonlinear Robot Manipulators

John M. Daly and David W. L. Wang

***Abstract*— This paper presents a novel bilateral teleoperation algorithm for n degree of freedom nonlinear manipulators connected through communication networks with time delays. Central to this approach is the use of second order sliding mode unknown input observers for estimating the external forces acting on the manipulators. The use of these observers removes the need for both velocity and force sensors, leading to a lower cost hardware setup that provides all of the advantages of a position-force teleoperation algorithm. A proof of stability for each of the master and slave manipulators and their associated observers and controllers is given, as well as stability results for the entire closed loop in the presence of time delays. Experimental results are presented, confirming the validity of this approach in practice.**

***Index Terms*— Bilateral teleoperation, sliding mode control, force estimation, sliding mode observers, time delays.**

I. Introduction

The field of teleoperation is one that has received much interest over the years, both from theoreticians and practitioners in control and robotics. One can envision many practical uses for teleoperation systems, such as interacting with harsh environments, telemedecine, and remote haptics. Of particular interest is bilateral teleoperation, which involves the ability to control a remote robot as well as to sense the forces acting on the robot in the remote environment. One of the major issues with time-delayed bilateral teleoperation is that of stability. Time delays are inherent in communication networks, and these time delays can lead to instability. This problem became evident to researchers early on in the teleoperation research [1]. Therefore, any bilateral teleoperation algorithm must focus on stability in the presence of delays.

In bilateral teleoperation, signals are transmitted from a master robot to a slave robot, and other signals are transmitted from the slave back to the master. Typically, a human operator uses the master manipulator, while the slave manipulator interacts with some remote environment. These signals pass through communications channels that, in general, cause time delays in the transmission. There are several different bilateral teleoperation architectures, including position-position and position-force architectures [2]. In a position-position architecture, the master manipulator position is transmitted to the slave, and the slave position is transmitted back to the master. The goal of this architecture is to have each side track the other. An issue with this approach is that differences between the master and slave position may be experienced as large reaction forces by the operator, even when the slave may be operating completely in free motion [2]. However, no force sensors are required. Niemeyer and Slotine [3], [4], [5], [6] have developed a well known variant of this architecture based on wave variables and ensuring passivity of the closed loop.

The position-force architecture involves transmitting the master position to the slave side and then a measurement of the slave environment force back from the slave to the master side. This additionally requires, at minimum, a force sensor mounted on the slave manipulator. However, the advantages of this architecture are perfect force tracking when the slave is in contact with an environment and a better perception of the system in free motion [7]. This increased performance, in terms of transparency, of the position-force architecture motivates research into position-force algorithms. However, force sensors can be costly and unreliable.

This paper presents a novel bilateral teleoperation algorithm for n degree of freedom (DOF) nonlinear robots that provides the benefits of a position-force architecture in terms of transparency and force tracking, but does not require the use of force sensors. The work presented here extends earlier work [8], which was developed for linear 1-DOF systems. As well, [8] makes use of first order sliding mode observers. The work presented here uses second order sliding mode observers [9], which are better suited to implementation on a computer in terms of the error due to a discrete implementation with a finite switching frequency. Unknown input sliding mode observers provide a useful framework for force estimation in robotics [8]. By treating the external forces acting on a manipulator as unknown inputs, those forces can be recovered by the observer in finite time.

In Section II the bilateral teleoperation system, along with associated controllers and observers, is presented. Section III presents the stability analysis of each of the master and slave systems, while Section IV develops stability results for the entire closed loop. An experimental verification is given in Section V. Conclusions and areas for future work are given in Section VI.

II. Problem Formulation

This bilateral teleoperation control algorithm uses force feedback with n-DOF master and slave manipulators at each side of the communications. Although similar to Cho *et al.* [10], which deals with linear 1-DOF systems and requires measurement of positions, velocities, and external forces, the algorithm presented here is developed for nonlinear n-DOF robots and requires only position measurements. A sliding mode controller is used at the slave side to ensure a desired

J. Daly and D. Wang are with the Department of Electrical and Computer Engineering, University of Waterloo, 200 University Avenue West, Waterloo, Ontario, Canada. jmdaly@ieee.org

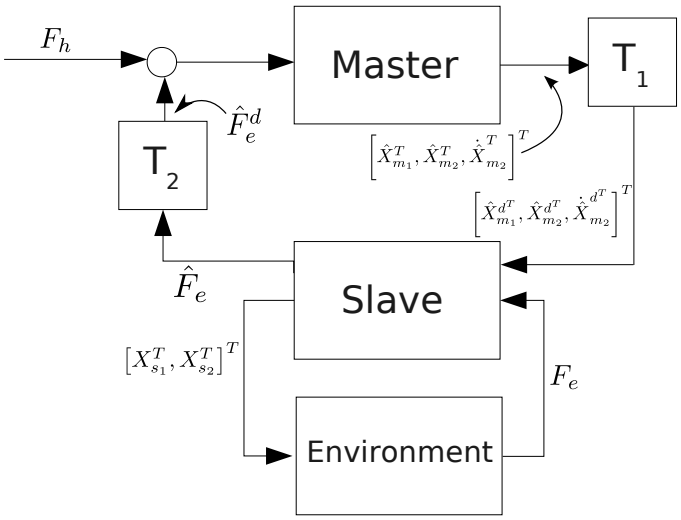

Fig. 1. Block diagram of the master system and the slave and environment subsystem.

closed loop impedance and tracking of the delayed master trajectory. A computed torque method impedance controller at the master side is used to give the master a desired impedance and to apply the reflected slave environment force back to the master. This is an output feedback algorithm, so robot position measurements drive observers that estimate both the state and the external forces. The control algorithm in this work is designed in the manipulator Cartesian space and the slave environment is modeled as an n-DOF system acting on the slave end effector. This is done since it is useful to be able to specify a desired impedance for each degree of freedom of the end effector. A block diagram representation of this system is given in Figure 1. In this diagram, the master block contains the master manipulator, observer, and controller, and likewise for the slave side. The inputs to the master system are the force F_h applied by the human operator and the delayed environment force estimate $\hat{F}_e^d$. The master trajectory estimate $[\hat{X}_{m_1}^T, \hat{X}_{m_2}^T, \dot{\hat{X}}_{m_2}^T]^T$ is transmitted through the delay T_1 to the slave. The slave interacts with the environment through its state output $[X_{s_1}^T, X_{s_2}^T]^T$, and receives as input the force F_e applied by the environment. Finally, the force estimate $\hat{F}_e$ exerted on the slave by the environment is reflected back to the master through delay T_2.

Consider the following master manipulator dynamics in joint space,

$$T_m = M_m(q_m)\ddot{q}_m + h_m(q_m, \dot{q}_m) - T_h \tag{1}$$

where $q_m \in R^n$ is the vector of joint positions, $T_m \in R^n$ is the vector of input torques, $M_m(q_m) \in R^{n\times n}$ is the mass matrix, $h_m(q_m, \dot{q}_m) \in R^n$ is a vector of other nonlinear terms, which could include gravity, Coriolis, and friction terms, and $T_h \in R^n$ is the vector of external torques applied by the human. Similarly, the slave dynamics in joint space are given as,

$$T_s = M_s(q_s)\ddot{q}_s + h_s(q_s, \dot{q}_s) + T_e \tag{2}$$

where q_s, T_s, $M_s(q_s)$, and $h_s(q_s, \dot{q}_s)$ are defined analogously to the master case, and $T_e \in R^n$ is the vector of external torques applied by the environment.

Control design will be performed in the robot task space. Following [11], it is straightforward to determine task space expressions for the robot dynamics. The master manipulator dynamics expressed in the robot task space are given as,

$$\begin{aligned} \dot{X}_{m_1} &= X_{m_2} && (3)\\ \dot{X}_{m_2} &= \bar{M}_m^{-1}(X_{m_1})\left(-\bar{h}_m(X_{m_1}, X_{m_2}) \right. \\ &\quad \left. + F_m + F_h\right) && (4) \end{aligned}$$

where $X_{m_1} \in R^n$ is the vector of positions and $X_{m_2} \in R^n$ is the vector of velocities. The matrices $\bar{M}_m(X_{m_1})$ and $\bar{h}_m(X_{m_1}, X_{m_2})$ are defined in [11]. Defining the slave states similarly, the slave state space representation of the dynamics is given as,

$$\begin{aligned} \dot{X}_{s_1} &= X_{s_2} && (5)\\ \dot{X}_{s_2} &= \bar{M}_s^{-1}(X_{s_1})\left(-\bar{h}_s(X_{s_1}, X_{s_2}) + F_s - F_e\right) && (6) \end{aligned}$$

Since this is an output feedback algorithm, observers are used at both the master and slave sites. These observers are based on the observer developed in [9], but are designed for the n-DOF case. They make use of the super-twisting second order sliding mode algorithm. Sliding mode observers are selected for several reasons. Their robustness properties to unmodeled dynamics are valuable in that the state estimates will converge to the true states in finite time despite the fact that the external force acting on the robot is not included in the observer dynamics. As well, this external force signal may be recovered from the equivalent output injection term in the observer. For the case of the n-DOF bilateral teleoperation system, MIMO observers are developed. The observer for the master robot is given as,

$$\begin{aligned} \dot{\hat{X}}_{m_1} &= \hat{X}_{m_2} + z_{m_1} && (7)\\ \dot{\hat{X}}_{m_2} &= \bar{M}_m^{-1}(\hat{X}_{m_1})\left(-\bar{h}_m(\hat{X}_{m_1}, \hat{X}_{m_2}) + F_m\right) \\ &\quad + z_{m_2} && (8) \end{aligned}$$

where $z_{m_1} \in R^n$ and $z_{m_2} \in R^n$. The i-th element of vector z_{m_1} is given as,

$$z_{m_{1i}} = \lambda_{m_i}|X_{m_{1i}} - \hat{X}_{m_{1i}}|^{1/2}\text{sign}(X_{m_{1i}} - \hat{X}_{m_{1i}}) \tag{9}$$

and the i-th element of vector z_{m_2} is given as,

$$z_{m_{2i}} = \alpha_{m_i}\text{sign}(X_{m_{1i}} - \hat{X}_{m_{1i}}) \tag{10}$$

where λ_{m_i} and α_{m_i} are constants whose values will be specified later. Note that the human force exerted on the end effector does not appear at all in the observer. Regardless of this, finite time convergence of the state estimates is

achieved, and an estimate of the human force is obtained as well. It is this force estimate that is used in the control law. The human force estimate is obtained from the equivalent output injection term $z_{m_{2i}}$ as,

$$\hat{F}_h = \bar{M}_m(\hat{X}_{m_1}) z_{m_2 eq} \tag{11}$$

where $z_{m_2 eq}$ represents a low pass filtering operation on z_{m_2} in order to obtain the equivalent output injection signal [12]. Note that, in practice, the above force estimate will contain all unmodeled terms in the manipulator dynamics. However, this work shows through experiments that with a suitable model of the manipulator dynamics, the recovered unknown input estimate is very usable as the force estimate. The second order sliding mode observer for the slave dynamics takes the same form as the master side observer. The equations for the slave observer are expressed as,

$$\dot{\hat{X}}_{s_1} = \hat{X}_{s_2} + z_{s_1} \tag{12}$$

$$\dot{\hat{X}}_{s_2} = \bar{M}_s^{-1}(\hat{X}_{s_1}) \left(-\bar{h}_s(\hat{X}_{s_1}, \hat{X}_{s_2}) + F_s \right) + z_{s_2} \tag{13}$$

where $z_{s_1} \in R^n$ and $z_{s_2} \in R^n$. The i-th element of vectors z_{s_1} and z_{s_2} are defined analogously to the i-th elements of z_{m_1} and z_{m_2}, respectively. The estimate of the environmental force acting on the slave is obtained from the equivalent output injection term $z_{s_2 i}$ as,

$$\hat{F}_e = -\bar{M}_s(\hat{X}_{s_1}) z_{s_2 eq} \tag{14}$$

Before presenting the master and slave controllers, some notation is introduced. A signal $x(t)$ delayed by T_1 seconds is represented as,

$$x^d(t) \equiv x(t - T_1)$$

Similarly, a signal delayed by two times delays, T_1 and T_2, is represented as,

$$x^{dd}(t) \equiv x(t - T_1 - T_2)$$

The master control law is a computed torque method controller to decouple and linearize each degree of freedom in the task space. The outer loop controller is specified as,

$$F_m = \bar{M}_m(\hat{X}_{m_1}) v_m + \bar{h}_m(\hat{X}_{m_1}, \hat{X}_{m_2}) - \hat{F}_h \tag{15}$$

The inner impedance controller, to provide each degree of freedom with desired impedance characteristics, is given as,

$$v_m = \tilde{M}_m^{-1} \left(-\tilde{B}_m \hat{X}_{m_2} - \tilde{K}_m \hat{X}_{m_1} + \hat{F}_h - \hat{F}_e^d \right) \tag{16}$$

where $\tilde{M}_m \in R^{n \times n}$ is the diagonal constant matrix that specifies the desired mass characteristic for each degree of freedom. The desired mass for the i-th degree of freedom is given by the i-th diagonal of $\tilde{M}_m$. The matrices $\tilde{B}_m \in R^{n \times n}$ and $\tilde{K}_m \in R^{n \times n}$ are also diagonal constant matrices representing the desired damping and stiffness values for each degree of freedom. The control law (15) and (16) ensures that, after convergence of the observers, the master manipulator has the desired mass-spring-damper impedance characteristics for each degree of freedom. As with any standard computed torque method controller, there will not be a perfect cancellation of nonlinearities in practice. However, for a robot modeled sufficiently well, this control technique provides desirable performance in practice, as will be shown in the experimental results.

Next, define the master-slave position and velocity tracking error as $e_{r_1} = X_{s_1} - X_{m_1}^d \in R^n$ and $e_{r_2} = X_{s_2} - X_{m_2}^d \in R^n$. The slave controller is designed in order to give each degree of freedom of the end effector a desired impedance characteristic. The n-DOF equation of dynamics that gives rise to the desired impedance is,

$$I = \tilde{M}_s \dot{e}_{r_2} + \tilde{B}_s e_{r_2} + \tilde{K}_s e_{r_1} + F_e = 0 \tag{17}$$

where the matrices $\tilde{M}_s$, $\tilde{B}_s$, and $\tilde{K}_s$ are defined as in the master controller, but for the slave impedances. When (17) is satisfied, the slave has the desired closed loop impedance and asymptotically tracks the delayed master trajectories. However, this work examines output feedback control. An output feedback version of the end effector dynamics that yield the desired impedance model is defined as,

$$\hat{I} = \tilde{M}_s \dot{\hat{e}}_{r_2} + \tilde{B}_s \hat{e}_{r_2} + \tilde{K}_s \hat{e}_{r_1} + \hat{F}_e = 0 \tag{18}$$

where $\hat{e}_{r_1} = \hat{X}_{s_1} - \hat{X}_{m_1}^d$ and $\hat{e}_{r_2} = \hat{X}_{s_2} - \hat{X}_{m_2}^d$. In order to ensure that this desired impedance characteristic is satisfied, the sliding surface for the slave controller is defined as,

$$\hat{s} = \int_0^t \tilde{M}_s^{-1} \hat{I}(\tau)\, d\tau \tag{19}$$

$$= \hat{e}_{r_2} + \int_0^t \left(\tilde{M}_s^{-1} \tilde{B}_s \hat{e}_{r_2} + \tilde{M}_s^{-1} \tilde{K}_s \hat{e}_{r_1} + \tilde{M}_s^{-1} \hat{F}_e \right) d\tau \tag{20}$$

$$= 0 \tag{21}$$

Then, the slave side sliding mode controller is given as,

$$\begin{aligned} F_s = & -\bar{M}_s(\hat{X}_{s_1}) \Big[\tilde{M}_s^{-1} \tilde{K}_s \hat{X}_{s_1} + \tilde{M}_s^{-1} \tilde{B}_s \hat{X}_{s_2} \\ & - \bar{M}_s^{-1}(\hat{X}_{s_1}) \bar{h}_s(\hat{X}_{s_1}, \hat{X}_{s_2}) \\ & + (\tilde{M}_m^{-1} \tilde{K}_m - \tilde{M}_s^{-1} \tilde{K}_s) \hat{X}_{m_1}^d \\ & + (\tilde{M}_m^{-1} \tilde{B}_m - \tilde{M}_s^{-1} \tilde{B}_s) \hat{X}_{m_2}^d - (\tilde{M}_m^{-1} \\ & - \bar{M}_m^{-1}(\hat{X}_{m_1}^d)) \hat{F}_h^d + \tilde{M}_m^{-1} \hat{F}_e^{dd} + \tilde{M}_s^{-1} \hat{F}_e + z_{s_2 eq} \\ & - z_{m_2 eq}^d + K_g \mathrm{sign}(\hat{s}) \Big] \end{aligned} \tag{22}$$

where $K_g = k_g I_{n \times n} \in R^{n \times n}$ and k_g is a scalar whose value will be specified later.

To summarize, for master robot (3), (4) and slave robot (5), (6) connected bilaterally through a time delay of T_1 seconds from the master to the slave and T_2 seconds from the slave to the master, the system may be controlled using the master control law (15) and (16) with master side observer

(7), (8) and slave sliding mode control law (22) with slave side observer (12), (13).

Having presented the bilateral teleoperation algorithm in its entirety, the next section will develop the stability analysis of this system.

III. Stability Analysis

In order to show stability of this system, the following assumption is made.

Assumption 3.1: The external forces acting on both master and slave are bounded for all time with some known upper bounds.

The observers used in this work are based on SISO observers presented in [9]. Here, MIMO observers are designed and a corollary is developed to demonstrate that the SISO observers may be extended to MIMO observers while still ensuring finite time convergence of the observer error dynamics to zero. This result is shown only for the master observer, but it is the same for the slave observer.

Define the observer estimation error as $\tilde{X}_{m_1} = X_{m_1} - \hat{X}_{m_1}$ and $\tilde{X}_{m_2} = X_{m_2} - \hat{X}_{m_2}$. Then, the observer error dynamics may be found as,

$$\begin{aligned} \dot{\tilde{X}}_{m_1} &= \tilde{X}_{m_2} - z_{m_1} && (23) \\ \dot{\tilde{X}}_{m_2} &= F(X_{m_1}, X_{m_2}, \hat{X}_{m_1}, \hat{X}_{m_2}, F_m, F_h) \\ &\quad -z_{m_2} && (24) \end{aligned}$$

where,

$$\begin{aligned} F(X_{m_1}, X_{m_2}, \hat{X}_{m_1}, \hat{X}_{m_2}, F_m, F_h) = \\ \bar{M}_m^{-1}(X_{m_1}) \left(-\bar{h}_m(X_{m_1}, X_{m_2}) + F_m + F_h\right) \\ -\bar{M}_m^{-1}(\hat{X}_{m_1}) \left(-\bar{h}_m(\hat{X}_{m_1}, \hat{X}_{m_2}) + F_m\right) \end{aligned}$$

and assume that the inequality, for the i-th element of F,

$$|F_i(X_{m_1}, X_{m_2}, \hat{X}_{m_1}, \hat{X}_{m_2}, F_m, F_h)| < f_i^+ \qquad (25)$$

for some constant f_i^+ holds over the operational domain. As long as the controller used stabilizes the process in the case of full state measurements, one can choose the observer error dynamics to be fast enough so that the state estimates are recovered before the robot leaves some chosen area. This will ensure that the bound (25) remains satisfied in the operational domain [9].

Let α_{m_i} and λ_{m_i} satisfy the following inequalities, for every element i in vectors α_m and λ_m respectively,

$$\begin{aligned} \alpha_{m_i} &> f_i^+ && (26) \\ \lambda_{m_i} &> \sqrt{\frac{2}{\alpha_{m_i} - f_i^+}} \frac{(\alpha_{m_i} + f_i^+)(1+p_i)}{(1-p_i)} && (27) \end{aligned}$$

Corollary 3.1: Suppose that the parameters for the observer (7) and (8) are selected according to the above conditions (26) and (27) for α_m and λ_m, and that condition (25) holds over the operational domain of the robot. Then, the variables of the observer converge in finite time to the states of the system, i.e. $(\hat{X}_{m_1}, \hat{X}_{m_2}) \to (X_{m_1}, X_{m_2})$. Further, the unknown force vector $F_h(t)$ may be recovered in finite time as $\bar{M}_m(\hat{X}_{m_1}) z_{m_{2eq}}$.

Proof: Omitted for space reasons. See [13]. The proof follows the SISO proof presented in [9]. ■

The next theorem shows asymptotic stability of both the master and slave under output feedback with force estimation, and in the presence of time delays in the communications.

Theorem 3.1: Consider master robot (3), (4) and slave robot (5), (6) connected bilaterally through a time delay of T_1 seconds from the master to the slave and T_2 seconds from the slave to the master, with master control law (15) and (16), master side observer (7), (8) and slave sliding mode control law (22) with slave side observer (12), (13). Then, there exists a sliding mode controller gain $K_g = k_g I_{n\times n}$ where,

$$k_g > ||z_{s_2} - z_{s_2eq} - z^d_{m_2} + z^d_{m_2eq}||_2 + \varepsilon_g \qquad (28)$$

for some $\varepsilon_g > 0$, and observer gains λ_m, α_m, λ_s, α_s such that the state estimates recover the true state in finite time, and the master and slave robot dynamics have the desired impedance model.

Proof: The first step is to show that the estimated states converge to the true states in finite time. Observer convergence for both the master and slave is guaranteed from Corollary 3.1, provided that the observer gains are chosen according to (26) and (27). The master observer states will be exactly the master states after T_m seconds, and likewise for the slave observer states after T_s seconds.

In order to show stability of the slave system, a Lyapunov function is used, and the controller is selected to ensure that the sliding mode dynamics are finite time stable. Due to the definition of the sliding surface (20), expressions for the dynamics of both the master and slave observers are required. The master observer dynamics, after substituting the master control law (15) and (16) into the original expression for the master observer dynamics (8), are given by,

$$\begin{aligned} \dot{\hat{X}}_{m_1} &= \hat{X}_{m_2} + z_{m_2} && (29) \\ \dot{\hat{X}}_{m_2} &= -\tilde{M}_m^{-1}\tilde{B}_m\hat{X}_{m_2} - \tilde{M}_m^{-1}\tilde{K}_m\hat{X}_{m_1} + \tilde{M}_m^{-1}\hat{F}_h \\ &\quad -\tilde{M}_m^{-1}\hat{F}_e^d - \bar{M}_m^{-1}(\hat{X}_{m_1})\hat{F}_h + z_{m_2} && (30) \end{aligned}$$

Substituting the delayed version of the closed loop master observer dynamics (30) and the slave observer dynamics (13) into the sliding surface (20) and simplifying, one arrives at,

$$\begin{aligned} \hat{s} = \int_0^t \Big(& -\bar{M}_s^{-1}(\hat{X}_{s_1})\bar{h}_s(\hat{X}_{s_1}, \hat{X}_{s_2}) + \tilde{M}_s^{-1}\tilde{K}_s\hat{X}_{s_1} \\ & +\tilde{M}_s^{-1}\tilde{B}_s\hat{X}_{s_2} - \tilde{M}_s^{-1}\tilde{K}_s\hat{X}^d_{m_1} - \tilde{M}_s^{-1}\tilde{B}_s\hat{X}^d_{m_2} \\ & + \tilde{M}_m^{-1}\tilde{K}_m\hat{X}^d_{m_1} + \tilde{M}_m^{-1}\tilde{B}_m\hat{X}^d_{m_2} \\ & -(\tilde{M}_m^{-1} - \bar{M}_m^{-1}(\hat{X}^d_{m_1}))\hat{F}_h^d + \tilde{M}_m^{-1}\hat{F}_e^{dd} \\ & +\tilde{M}_s^{-1}\hat{F}_e + \bar{M}_s^{-1}(\hat{X}_{s_1})F_s + z_{s_2} - z^d_{m_2} \Big)\, d\tau \qquad (31) \end{aligned}$$

Now consider the Lyapunov function candidate,

$$V_s = \frac{1}{2}\hat{s}^T\hat{s} \tag{32}$$

Taking the derivative of V_s along the trajectories of the system,

$$\begin{aligned}\dot{V}_s &= \hat{s}^T\dot{\hat{s}} &(33)\\ &= \hat{s}^T\Big[\Big(-\bar{M}_s^{-1}(\hat{X}_{s_1})\bar{h}_s(\hat{X}_{s_1},\hat{X}_{s_2}) + \tilde{M}_s^{-1}\tilde{K}_s\hat{X}_{s_1}\\ &\quad +\tilde{M}_s^{-1}\tilde{B}_s\hat{X}_{s_2} - \tilde{M}_s^{-1}\tilde{K}_s\hat{X}^d_{m_1} - \tilde{M}_s^{-1}\tilde{B}_s\hat{X}^d_{m_2}\\ &\quad +\tilde{M}_m^{-1}\tilde{K}_m\hat{X}^d_{m_1} + \tilde{M}_m^{-1}\tilde{B}_m\hat{X}^d_{m_2}\\ &\quad -(\tilde{M}_m^{-1} - \bar{M}_m^{-1}(\hat{X}^d_{m_1}))\hat{F}^d_h + \tilde{M}_m^{-1}\hat{F}^{dd}_e\\ &\quad +\tilde{M}_s^{-1}\hat{F}_e + \bar{M}_s^{-1}(\hat{X}_{s_1})F_s + z_{s_2} - z^d_{m_2}\Big)\Big] &(34)\end{aligned}$$

Now simplifying (22) and (34) and noting that $\hat{s}^T\text{sign}(\hat{s}) = \sum_{i=1}^n |\hat{s}_i| = ||\hat{s}||_1$ yields,

$$\dot{V}_s \leq -k_g||\hat{s}||_1 + |\hat{s}^T\left(z_{s_2} - z_{s_2eq} - z^d_{m_2} + z^d_{m_2eq}\right)|$$

The second term on the right hand side of the above inequality represents an inner product of two vectors. By the Cauchy-Schwartz inequality and recalling that $||x||_2 \leq ||x||_1$ in R^n leads to,

$$\begin{aligned}\dot{V}_s &\leq -k_g||\hat{s}||_1 + ||\hat{s}||_1\,||z_{s_2} - z_{s_2eq} - z^d_{m_2} + z^d_{m_2eq}||_2\\ &= -||\hat{s}||_1\left(k_g - ||z_{s_2} - z_{s_2eq} - z^d_{m_2} + z^d_{m_2eq}||_2\right)\end{aligned}$$

Choosing k_g as in (28) ensures that,

$$\dot{V}_s < -||\hat{s}||_1\varepsilon_g < 0 \qquad \forall\,||\hat{s}||_1 \neq 0 \tag{35}$$

This guarantees stability, and additionally finite time convergence of the system trajectories to the sliding surface. Finite time convergence is shown through the Comparison Lemma [14]. As long as k_g is chosen large enough, the sliding surface will be reached in T_g seconds.

Satisfying the conditions of Corollary 3.1 ensures that both the master and slave estimation errors will converge to zero within T_m seconds and T_s seconds, respectively. As well, the system trajectories will reach the sliding surface $\hat{s} = 0$ within T_g seconds. Therefore, at $t = \max(T_s, T_m, T_g)$, all observers will have converged, the slave dynamics will reach the sliding surface $\hat{s} = 0$, and all force estimates will be equal to the actual external forces acting on the robots.

One may compute the slave equivalent control signal by solving for the control input in the equation $\dot{\hat{s}} = 0$. Finding the equivalent control and substituting it into the slave dynamics (5), (6) once the observers have converged yields,

$$\begin{aligned}\dot{X}_{s_1} &= X_{s_2} &(36)\\ \dot{X}_{s_2} &= -\tilde{M}_s^{-1}\tilde{K}_sX_{s_1} - \tilde{M}_s^{-1}\tilde{B}_sX_{s_2} - \tilde{M}_s^{-1}F_e\\ &\quad +\dot{X}^d_{m_2} + \tilde{M}_s^{-1}\tilde{B}_sX^d_{m_2} + \tilde{M}_s^{-1}\tilde{K}_sX^d_{m_1} &(37)\end{aligned}$$

Next, the closed loop expression for the master dynamics is found by substituting the master controller (15) and (16) into the master robot dynamics (3) and (4). Making this substitution and simplifying yields,

$$\begin{aligned}\dot{X}_{m_1} &= X_{m_2} &(38)\\ \dot{X}_{m_2} &= -\tilde{M}_m^{-1}\tilde{K}_mX_{m_1} - \tilde{M}_m^{-1}\tilde{B}_mX_{m_2} + \tilde{M}_m^{-1}F_h\\ &\quad -\tilde{M}_m^{-1}F^d_e &(39)\end{aligned}$$

In order to determine the tracking error dynamics $e_{r_1} = X_{s_1} - X^d_{m_1}$ and $e_{r_2} = X_{s_s} - X^d_{m_2}$, subtract the delayed version of (38) from (36) and the delayed version of (39) from (37). This yields,

$$\begin{aligned}\dot{e}_{r_1} &= e_{r_2} &(40)\\ \dot{e}_{r_2} &= -\tilde{M}_s^{-1}\tilde{K}_se_{r_1} - \tilde{M}_s^{-1}\tilde{B}_se_{r_2} - \tilde{M}_s^{-1}F_e &(41)\end{aligned}$$

This result is exactly the equation of dynamics representing the desired characteristic impedance for the tracking error dynamics. This analysis has shown that on the sliding surface the master and slave dynamics remain stable, and the desired characteristic impedance is achieved.

■

Theorem 3.1 guarantees stability of each of the master and slave robots. However, stability of the entire closed loop is not addressed in this result. The next section addresses the issue of closed loop stability when the slave is in contact with an environment.

IV. Closed Loop Stability

Having guaranteed stability for each of the master and slave manipulators with their associated observers and controllers, it remains to show that the entire closed loop can be stabilized in the presence of time delays. This section will present closed loop stability results for the case where the environment is a nonlinear finite-gain stable system.

In general, one may not be able to assume a known structure for the slave side environment. In fact, it may not even be possible to determine one. This section will show that, for a general nonlinear environment with a finite gain and a small modification to the slave closed loop dynamics, stability independent of delay for an unknown nonlinear environment may be achieved.

Defining the environment as some relation,

$$F_e = HX_s \tag{42}$$

where $H : L^{2n}_{2e} \to L^n_{2e}$ is the mapping relating slave state to environmental force, this subsystem must be finite-gain L_2 stable. That is, there must exist nonnegative constants γ_e and β_e such that,

$$||(HX_s)_\tau||_{L_2} \leq \gamma_e||(X_s)_\tau||_{L_2} + \beta_e \tag{43}$$

for all $X_s \in L^{2n}_{2e}$ and $\tau \in [0, \infty)$.

One would like to be able to choose the slave robot L_2 gain arbitrarily small to ensure a loop gain of less than

one. However, the H_∞ norm of the slave system cannot be made arbitrarily small without some modification. In order to overcome this, a scaling term k_p on the delayed master states is introduced. As well, the desired impedance parameters are re-defined. Define,

$$\tilde{M}_s = \epsilon_p \tilde{M}'_s,\ \tilde{B}_s = \epsilon_p \tilde{B}'_s,\ \tilde{K}_s = \epsilon_p \tilde{K}'_s \tag{44}$$

where ϵ_p is a positive scalar to be set by the designer and $\tilde{M}'_s$, $\tilde{B}'_s$, and $\tilde{K}'_s$ are positive diagonal matrices that may be freely chosen as well. Introducing these parameters has the effect of giving full control of the H_∞ norm of the slave to the designer while maintaining the desired dynamic behaviour. Introducing the scalar master trajectory scaling factor k_p and using the re-definitions of the impedance parameters, one can express the slave dynamics as,

$$\begin{bmatrix} \dot{X}_{s_1} \\ \dot{X}_{s_2} \end{bmatrix} = \underbrace{\begin{bmatrix} 0 & I_{n\times n} \\ -\tilde{M}_s^{'-1}\tilde{K}'_s & -\tilde{M}_s^{'-1}\tilde{B}'_s \end{bmatrix}}_{A_s} \begin{bmatrix} X_{s_1} \\ X_{s_2} \end{bmatrix} +$$

$$\underbrace{\begin{bmatrix} 0 & 0 & 0 & 0 \\ k_p\tilde{M}_s^{'-1}\tilde{K}'_s & k_p\tilde{M}_s^{'-1}\tilde{B}'_s & k_p I_{n\times n} & -\epsilon_p^{-1}\tilde{M}_s^{'-1} \end{bmatrix}}_{B_s}$$

$$\times \begin{bmatrix} X^d_{m_1} \\ X^d_{m_2} \\ \dot{X}^d_{m_2} \\ F_e \end{bmatrix} \tag{45}$$

$$Y_s = \underbrace{\begin{bmatrix} I_{n\times n} & 0 \\ 0 & I_{n\times n} \end{bmatrix}}_{C_s} \begin{bmatrix} X_{s_1} \\ X_{s_2} \end{bmatrix} \tag{46}$$

Lemma 4.1: Given the slave system (45) and (46) with the scaling factor k_p on the delayed master trajectory inputs, set $\tilde{K}_s = \epsilon_p \tilde{K}'_s$, $\tilde{B}_s = \epsilon_p \tilde{B}'_s$, and $\tilde{M}_s = \epsilon_p \tilde{M}'_s$. Then, the H_∞ norm of the slave system may be made arbitrarily small.

Proof: Omitted for space. See [13]. ■

Lemma 4.2: Consider master system (38) and (39) connected through time delays to slave system (36) and (37). Define the gain of the slave-environment subsystem as γ_{s+e} and the gain of the master system as γ_m. If the master impedance parameters are chosen as,

$$m_{m_i} > \gamma_{s+e}\sqrt{\frac{3}{2}},\ k_{m_i} = m_{m_i},\ b_{m_i} = \sqrt{2k_{m_i}m_{m_i}} \tag{47}$$

then the loop gain $\gamma_m\gamma_{s+e}$ always satisfies the condition $\gamma_m\gamma_{s+e} < 1$.

Proof: Omitted for space. See [13]. ■

Theorem 4.1: Consider the finite-gain stable environment operator (42), with known gain γ_e, connected in feedback with the slave subsystem (45) and (46). One can always ensure that this feedback connection is finite-gain stable by ensuring that the slave L_2 gain $\gamma_s < 1/\gamma_e$.

Proof: By Lemma 4.1 one can choose slave parameters such that γ_s may be made arbitrarily small. The condition $\gamma_s < 1/\gamma_e$ may be equivalently expressed as,

$$\gamma_s\gamma_e < 1 \tag{48}$$

This is a small gain condition. When (48) is satisfied, the slave-environment loop is finite-gain L_2 stable by the Small Gain Theorem [14]. ■

The slave-environment closed loop gain is defined as γ_{s+e}. It has already been shown in Lemma 4.2 that a suitable choice of master robot parameters may always be made to ensure the closed-loop stability of the master-slave system. In this case one can choose parameters to ensure that,

$$||G_m(s)||_\infty < \frac{1}{\gamma_{s+e}} \tag{49}$$

Then the feedback connection of the finite-gain L_2 stable master with the finite-gain L_2 stable slave+environment subsystem is guaranteed to be stable by the Small Gain Theorem. Note that delay elements have a gain of one and so delays of this nature do not affect stability of the closed loop when the small gain condition is met.

Other results have been developed for linear environments that allow for less conservative choices of the closed loop impedance parameters. As well, a closed loop stability result has been developed for the case when the human is also modeled as nonlinear dynamics. This work is detailed in [13].

V. Experimental Results

While the algorithm presented has been shown to be stable theoretically, it is important to ensure that the approach is feasible in practice. The experimental implementation involves factors not addressed in the theory, namely unmodeled dynamics, friction, sensor noise, and a limited sample period.

This algorithm is implemented on the University of Waterloo Teleoperation Platform, which consists of two 3-DOF robot manipulators connected to a PC through data acquisition hardware. Only the revolute base degree of freedom is used on each robot, while the other degrees of freedom are locked. In performing 1-DOF experiments, one can show that the algorithm is implementable in practice and robust to real world issues such as unmodeled dynamics and sensor noise. Future work will implement these algorithms on higher degree of freedom robots. There are position encoders on each motor for position measurements, but no velocity sensors exist. Dynamic models of the base degree of freedom for each manipulator were developed prior to running the experiments. For each robot, the base degree of freedom was modeled as a mass-damper with Coulomb friction. The master robot dynamics are given as,

$$\dot{x}_{m_1} = x_{m_2} \tag{50}$$

$$\dot{x}_{m_2} = -\frac{B_m}{J_m}x_{m_2} - \frac{1}{J_m}f_{cm}(x_{m_2}) + \frac{1}{J_m}F_h + \frac{1}{J_m}F_m \tag{51}$$

where,

$$f_{cm}(x_{m_2}) = \begin{cases} f_{cm1} & \text{if } x_{m_2} \geq 0 \\ f_{cm2} & \text{if } x_{m_2} < 0 \end{cases}$$

A system identification was performed for this manipulator, giving the following values for the parameters: $J_m = 0.8084$, $B_m = 0.1150$, $f_{cm1} = 0.1090$, and $f_{cm2} = -0.0746$. Similarly, the slave dynamic model is given as,

$$\dot{x}_{s_1} = x_{s_2} \tag{52}$$

$$\dot{x}_{s_2} = -\frac{B_s}{J_s}x_{s_2} - \frac{1}{J_s}f_{cs}(x_{s_2}) - \frac{1}{J_s}F_e + \frac{1}{J_s}F_s \tag{53}$$

where,

$$f_{cs}(x_{s_2}) = \begin{cases} f_{cs1} & \text{if } x_{s_2} \geq 0 \\ f_{cs2} & \text{if } x_{s_2} < 0 \end{cases}$$

Identifying the slave parameters yields the following values: $J_s = 0.8042$, $B_s = 0.1768$, $f_{cs1} = 0.1462$, and $f_{cs2} = -0.0237$.

Note that since the robots are 1-DOF manipulators there is no need to transform the system to the Cartesian space, and all control design may be performed directly in the joint space.

Due to limitations of the hardware used, the sample time in the experiments is limited to $T_s = 5 \times 10^{-4}$ seconds, giving a sample frequency of 2 kHz. As well, the position encoders produce signals with some noise. This can be a complication with sliding mode observers in practice. As a result, the pure switching components in the observers were replaced by saturation functions, which allow the use of a boundary layer. This boundary layer reduces the effect of chattering and provides more usable state estimates. It was determined experimentally that boundary layer widths of $\epsilon_m = 10^{-4}$ and $\epsilon_s = 10^{-2}$, for the master and slave observers respectively, yielded the best state estimates in terms of reducing chattering. The observer gain parameters were chosen experimentally to ensure that the second order sliding mode gain conditions are met and that good state estimates are produced. The observer gains are set to $\lambda_m = 10.5$, $\alpha_m = 15.4$ for the master observer, and $\lambda_s = 10.5$, $\alpha_s = 15.4$ for the slave as well. In order to obtain the estimated force signals from the observers, the switching signals were passed through 5 Hz second order low pass filters. This filtering yielded very usable force estimates.

It was also found in practice that the use of a pure switching component in the slave control signal produced significant chattering in the manipulator. As a result, a boundary layer was used in the slave sliding mode controller. As well, the slave control signal was passed through a second order low pass filter before being applied to the robot. Without the use of the filter, the chattering became too great, causing too much power draw through the motor amplifier power supply.

A very stiff metal structure was used as the environment at the slave side. However, the last link on the manipulator (the link that contacts the environment) is a link with some flexibility, giving some compliance to the manipulator-environment interface. The flexible link on the slave robot has a modulus of elasticity of 69×10^5 N-cm^2 [15]. The environment dynamics are not specifically modeled, but closed loop impedance parameters were chosen experimentally to ensure stable behaviour in contact.

For the experiment, the master closed loop impedance parameters were chosen as $\tilde{M}_m = 22$, $\tilde{B}_m = 32$, and $\tilde{K}_m = 22$. The slave closed loop impedance parameters were chosen as $\tilde{M}_s = 7$, $\tilde{B}_s = 42$, $\tilde{K}_s = 63$. While in practice these spring parameters are fairly large, but suitably chosen for this experimental setup, to ensure slave tracking stability one need only choose a slave side spring force that is positive. The slave values were chosen to give the slave manipulator, and by extension the tracking error dynamics, a pair of critically damped poles at $s = -3$. The master impedance parameters were chosen such that the closed loop system would be stable independent of delay by the Small Gain Theorem. The slave control signal was filtered with a second order low pass 25 Hz filter. Time delays of 0.5 seconds were introduced from the master to the slave side, and from the slave back to the master.

Figure 2 shows the master and the slave trajectories for this experiment. In the presence of time delays, the system remains stable both in and out of contact with the environment. There is some small error in tracking when the slave is in free motion. Several factors may contribute to this. The first is modeling error. It is apparent that there is some static friction in the system that has not been modeled, causing a non-zero position error in steady state since not enough control effort is being applied to overcome the static friction. As well, there is certainly some error on the inertial and damping parameter values in the identified robot models. An additional source of error is due to the fairly large boundary layer that is used in the sliding mode controller. This contributes to tracking error, as the sliding surface $s = 0$ is never actually reached. There are some small periods of time where the slave manipulator experiences some chattering. This is likely caused by the noise on the state and force estimates due to running the observers at a larger than ideal sample period. However, it is not significant in this experiment.

The estimate of the torque applied to the master manipulator is given in Figure 3. Due to the spring term on the master manipulator, which is a requirement for the closed loop stability analysis, the human operator must always apply a non-zero force to the manipulator when it is away from the origin. In practice, it is desirable to set the spring term to zero, or close to zero, on the master side as this gives the operator the sensation of using a tool that can be arbitrarily placed in the space and left there. It is also apparent in Figure 3 that during periods of time when the slave manipulator is in contact with the environment, the operator must apply more torque to the master manipulator to compensate for the environment torque that is fed back to the master from the slave. This further shows the effectiveness of the the algorithm, even with a round trip delay of 1 second.

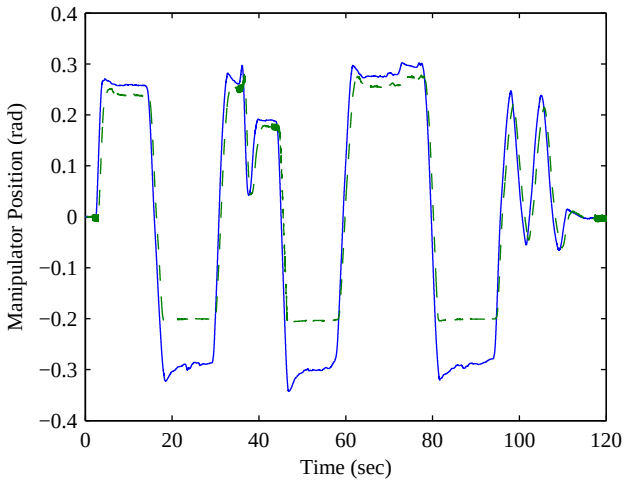

Fig. 2. Position of the master (solid) and slave (dashed) manipulators in the second experiment.

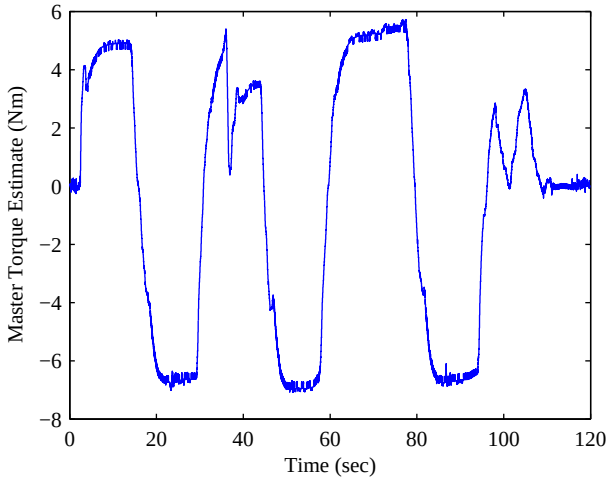

Fig. 3. Estimate of the human torque applied to the master in the second experiment.

VI. Conclusion

This paper has presented a novel bilateral teleoperation algorithm for n-DOF nonlinear robot manipulators connected through time delays. The algorithm provides the benefits of a position-force teleoperation architecture while only requiring position measurements. This effectively gives the advantages of both the position-position and position-force architectures while removing their respective disadvantages. Using unknown input sliding mode observers, both the external forces and robot states are estimated exactly with finite time convergence, thus eliminating the need for velocity and force sensors. The output feedback controllers for each of the master and slave decouple and linearize the dynamics in the Cartesian space, allowing one to specify desired impedance characteristics for each end effector DOF.

Closed loop stability of the whole teleoperator system under time delays has been proved for a nonlinear slave side environment.

This paper has also shown experimental results for the proposed algorithm. In particular, since sliding mode techniques have been used in the algorithm, it is important to verify that these approaches will work even though it was necessary to use a slower sample frequency than is desirable for the sliding mode observers, due to hardware limitations. However, with the use of boundary layers in the slave controller and the observers, as well as with some filtering of the slave control signal, a feasible and practical implementation of this algorithm can be achieved. Both tracking of the master by the slave and force reflection from the slave back to the master were effectively demonstrated. This result represents a new position-force teleoperation architecture without the need for force sensing.

Additionally, the experimental results suggest that this algorithm is stable through contact transitions at the slave side. This is one aspect to be examined from a theoretical standpoint in future work. An important area for future work would be to implement this algorithm on hardware that allows for faster sample frequencies and on manipulators that have less friction in order to see even better results in practice.

References

[1] W. R. Ferrell, "Delayed force feedback," *IEEE Transactions on Human Factors in Electronics*, vol. HFE-8, pp. 449–455, Oct. 1966.

[2] D. A. Lawrence, "Stability and transparency in bilateral teleoperation," *IEEE Transactions on Robotics and Automation*, vol. 9, no. 5, pp. 624–637, Oct. 1993.

[3] G. Niemeyer and J.-J. E. Slotine, "Towards force-reflecting teleoperation over the internet," in *Proceedings of the 1998 IEEE International Conference on Robotics & Automation*, May 1998.

[4] ——, "Telemanipulation with time delays," *The International Journal of Robotics Research*, vol. 23, pp. 873–890, Sept. 2004.

[5] ——, "Stable adaptive teleoperation," *IEEE Journal of Oceanic Engineering*, vol. 16, no. 1, pp. 681–694, Jan. 1991.

[6] ——, "Designing force reflecting teleoperators with large time delays to appear as virtual tools," in *Proceedings of the 1997 IEEE International Conference on Robotics & Automation*, Apr. 1997.

[7] M. Tavakoli, A. Aziminejad, R. V. Patel, and M. Moallem, "Enhanced transparency in haptics-based master-slave systems," in *Proceedings of the 2007 American Control Conference*, July 2007.

[8] J. M. Daly and D. W. L. Wang, "Bilateral teleoperation using unknown input observers for force estimation," in *Proceedings of the 2009 American Control Conference*, June 2009.

[9] J. Davila, L. Fridman, and A. Levant, "Second-order sliding-mode observer for mechanical systems," *IEEE transactions on automatic control*, vol. 50, no. 11, pp. 1785–1789, 2005.

[10] H. C. Cho, J. H. Park, K. Kim, and J.-O. Park, "Sliding-mode-based impedance controller for bilateral teleoperation under varying time delay," in *Proceedings of the 2001 IEEE International Conference on Robotics & Automation*, May 2001.

[11] M. W. Spong and M. Vidyasagar, *Robot Dynamics and Control*. United States of America: John Wiley & Sons, Inc., 1989.

[12] S. Drakunov and V. Utkin, "Sliding mode observers. tutorial." in *Proceedings of the 34th Conference on Decision & Control*, Dec. 1995, pp. 3376–3378.

[13] J. M. Daly, "Output feedback bilateral teleoperation with force estimation in the presence of time delays," PhD Dissertation, University of Waterloo, Waterloo, Ontario, Apr. 2010.

[14] H. K. Khalil, *Nonlinear Systems*, 3rd ed. New Jersey: Prentice Hall Inc., 2002.

[15] D. R. Madill, "Modelling and control of a haptic interface: A mechatronics approach," PhD Dissertation, University of Waterloo, Waterloo, Ontario, 1998.